Tetrahedron 64 (2008) 10754–10760

Contents lists available at ScienceDirect

Tetrahedron

journal homepage: www.elsevier.com/locate/tet

Photochemistry of 3,6-bis(styryl)pyridazines in solution and in neat liquid crystalline phase—optical switching and imaging techniques

Herbert Meier *, Thorsten Lifka, Peter Seus, Annette Oehlhof, Sabine Hillmann

Institute of Organic Chemistry, University of Mainz, Duesbergweg 10-14, 55099 Mainz, Germany

ARTICLE INFO

Article history:
Received 27 May 2008
Received in revised form 20 August 2008
Accepted 25 August 2008
Available online 30 August 2008

Keywords:
E/*Z* Isomerization
Liquid crystals
Phase behavior
Triplet quencher
Triplet sensitizer

ABSTRACT

3,6-Bis(styryl)pyridazines **1a**–**f** with 2–6 alkoxy groups show on irradiation in solution a stereoisomerization which leads to a photostationary state of (*E*,*E*)- and (*E*,*Z*)-isomer. Sensitizing and quenching experiments reveal that the (*E*,*E*)→(*E*,*Z*) route is a pure triplet process, whereas the (*E*,*Z*)→(*E*,*E*) route can have a minor singlet by-reaction.

Hexyloxy or dodecyloxy chains on the terminal benzene rings convey the (*E*,*E*)-isomers of compounds **1a**,**b**,**d**–**f** thermotropic liquid crystalline properties. In particular S_A, S_C, and $S_{F/I}$ phases were studied with regard to their photochemical behavior. Depending on the system, photodegradation of the smectic phase to the isotropic melt (S→I) or photoinduction of the smectic phase (I→S) can be achieved by alteration of the (*E*,*E*)/(*E*,*Z*) ratio. These processes represent the basis for imaging techniques (writing and erasing of information).

1. Introduction

Stilbenoid systems represent a highly interesting class of compounds in materials science and photochemistry. Their chromophores/fluorophores/electrophores have tunable properties for many technical applications.[1] Whereas, the number of publications and patents on oligomers and polymers consisting of (*E*)-stilbene building blocks is huge, there are comparably few studies on analogous compounds, which contain azine rings (pyridine, pyridazine, pyrimidine, pyrazine, triazine, tetrazine) instead of benzene rings (Scheme 1).[2,20]

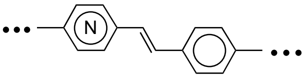

Scheme 1. Stilbenoid building blocks, which contain heteroaromatic six rings with 1–4 nitrogen atoms.

We prepared recently (*E*,*E*)-3,6-bis(styryl)pyridazines **1**, which represent ideal mesogens for photosensitive liquid crystals.[2a] The incorporated nitrogen atoms bear free electron pairs, which enable $n\rightarrow\pi^*$ transitions in addition to the usual $\pi\rightarrow\pi^*$ transitions in the electron excitation of stilbenoid compounds. Unsubstituted pyridazine shows the allowed $\pi\rightarrow\pi^*$ transition at a λ_{max} value of 246 nm and the $n\rightarrow\pi^*$ transition at λ_{max}=313 nm (measurement in ethanol).[3] (*E*)-3-Styrylpyridazine has a strong red-shifted $\pi\pi^*$ band with λ_{max}=290 nm and a shoulder for the $n\rightarrow\pi^*$ transition at 350 nm (measurement in *n*-heptane).[4] In addition to the internal conversion (IC) $S_2(n^2\_\pi\pi^*)\rightarrow S_1(n\_\pi^2\pi^*)\rightarrow S_0(n^2\_\pi^2)$ intersystem crossing (ISC) to the triplet state has to be faced: $S_1(n\_\pi^2\pi^*)\rightarrow T_2(n^2\_\pi\pi^*)$ and $S_2(n^2\_\pi\pi^*)\rightarrow T_1(n\_\pi^2\pi^*)$. According to El-Sayed's rule,[5,6] first-order spin-orbit couplings make the ISC $S_1\rightarrow T_2$ and $S_2\rightarrow T_1$ allowed, whereas the processes $S_1\rightarrow T_1$ and $S_2\rightarrow T_2$ are forbidden. The triplet states have their own typical photophysics and photochemistry. We expect efficient isomerizations $E\leftrightarrows Z$ on irradiation of such systems—even when the chromophores have an extended conjugation. In 1,4-distyrylbenzenes and higher oligo(1,4-phenylenevinylene)s [OPVs] such stereoisomerizations do not take place in the $E\rightarrow Z$ direction.[7] The bond orders of the olefinic double bonds are too high for a rotation in the excited singlet state S_1 and an ISC to the triplet state T_1 does virtually not occur.[7,8]

Reversible (*E*,*E*)⇆(*E*,*Z*) isomerizations should certainly be the prevailing photoreactions of the (*E*,*E*)-3,6-bis(styryl)pyridazines **1** in solution. Moreover, the present study has the aim to find out, if such optical switching processes are principally working in the LC phases of **1** and how their efficiency depends on the molecular order in these LC phases, which represent constrained media for the involved electronically excited particles.

A certain amount of (*E*,*Z*) configurations of **1** should lead to the breakdown of the liquid crystal, which then should be restored, when the reverse photoreaction (*E*,*Z*)-**1**→(*E*,*E*)-**1** provokes, that the

---

* Corresponding author. Fax: +49 6131 3925396.
E-mail address: hmeier@mail.uni-mainz.de (H. Meier).

0040-4020/$ – see front matter © 2008 Published by Elsevier Ltd.
doi:10.1016/j.tet.2008.08.075

portion of 'wrong' configuration falls below the critical percentage.[9] Some (*E*,*Z*) configurations can certainly be tolerated by a not very highly ordered liquid crystal—in particular at the domain borders.

2. Results and discussion

2.1. UV–vis absorption and formation of triplet states

Scheme 2 shows the di-, tetra-, and hexaalkoxy substituted (*E*,*E*)-3,6-distyryl-pyridazines **1a**–**f**, which we are discussing here. Their preparation and their mesophases were described earlier.[2a]

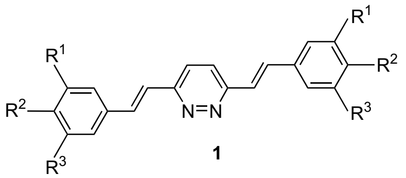

1

1	R^1	R^2	R^3
a	H	OC_6H_{13}	H
b	H	OC_6H_{13}	OC_6H_{13}
c	OC_6H_{13}	OC_6H_{13}	OC_6H_{13}
d	H	$OC_{12}H_{25}$	H
e	H	$OC_{12}H_{25}$	$OC_{12}H_{25}$
f	$OC_{12}H_{25}$	$OC_{12}H_{25}$	$OC_{12}H_{25}$

Scheme 2. Alkoxy substituted 3,6-bis(styryl)pyridazines **1a**–**f**.

Compounds **1a**–**f** have the character of donor–acceptor–donor systems[9] and exhibit a strong long-wavelength absorption between 280 and 420 nm. [ε_{max}=(5±0.3)10^4]. Table 1 summarizes their λ_{max} values. Number and length of the side chains have a small influence on the absorption. The absorption bands do not have a vibrational structure at room temperature and they do not reveal the position of the hidden $n_-\rightarrow\pi^*$ transition. A strong indication for the participation of the latter transition is the fact, that none of the compounds shows a fluorescence $S_1(\pi\pi^*)\rightarrow S_0(\pi^2)$, whereas the corresponding 1,4-bis(styryl)benzenes have high fluorescence quantum yields ($\phi_F\approx$0.8–0.9).[10,11]

In order to get an idea of the forbidden $n_-\rightarrow\pi^*$ transitions, we calculated the electron excitations of compounds **1′a**–**f**, in which the OR groups of **1a**–**f** are replaced by OH. The olefinic double bonds of **1**/**1′** can have a *transoid* and two different *cisoid* arrangements. Rotation of the terminal phenyl groups leads for **1b**,**e**/**1′b**,**e** to 10 planar rotamers, whereas **1a**,**c**,**d**,**f**/**1′a**,**c**,**d**,**f** have 3 planar conformers, each. Force field calculations MMX furnished the geometries of these conformers, which then served as structural basis for CNDO/CI calculations of the electron excitations. Figure 1 shows four selected orbitals of **1′a**, which proved to be important for the electron transitions. The configuration interaction reveals that the allowed $\pi\rightarrow\pi^*$ transition is to 90% a HOMO→LUMO transition and represents the energy-lowest transition. The $n_-\rightarrow\pi^*$ transition (Fig. 1) has a somewhat higher energy and consists mainly (70%) of the transition HOMO-6→LUMO+2. The calculated λ_{values} listed in Table 1 are average values for the possible conformers, which differ among each other by almost ±8 nm. The MMX/CNDO/CI calculations of the other compounds **1′** gave quite similar results: the $\pi\rightarrow\pi^*$ (HOMO→LUMO) transitions have somewhat lower energy than the $n_-\rightarrow\pi^*$ transitions. The number of OH groups has a very small influence on the electron transition energy.[12] Additional vibrational energy should in any case enable internal conversions (ICs) between $\pi\pi^*$ and $n\pi^*$ singlet states and subsequent intersystem crossings (ISCs) to T_1 or T_2 (Fig. 2).[13]

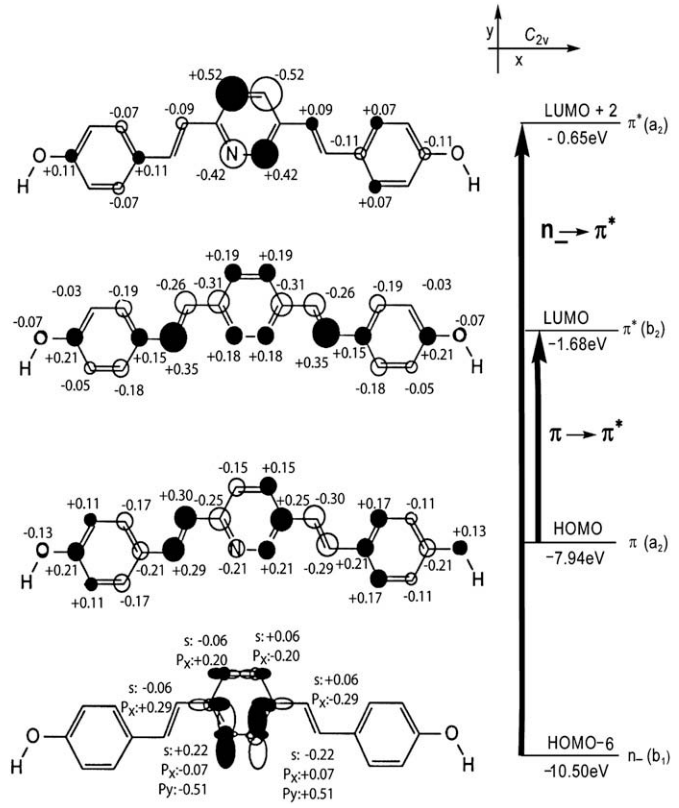

Figure 1. Selected orbitals (CNDO/CI calculation) of **1′a** (*cisoid* conformation with olefinic double bonds, which are *syn*-oriented to the N atoms). The numbers refer to the atomic p_z coefficients: +●, −○, and for HOMO-6 to the s, p_x, and p_y coefficients.

Table 1
Long-wavelength absorption maxima of the (*E*,*E*)-3,6-bis(styryl)pyridazines **1a**–**c** (measured in cyclohexane) and **1d**–**f** (measured in dichloromethane) and calculated λ_{max} values of the corresponding hydroxy compounds **1′a**–**f** (gas phase)

Compound **1**	λ_{max} [nm] $\pi\rightarrow\pi^*$	Compound **1′**	λ_{max} [nm] $\pi\rightarrow\pi^*$	$n\rightarrow\pi^*$
a	365	**a**	344	324
b	376	**b**	347	323
c	372	**c**	344	323
d	369	**d**	344	324
e	380	**e**	347	323
f	376	**f**	344	323

2.2. Photochemistry in solution

An efficient intersystem crossing (ISC) to the triplet state is a precondition for a reversible *E*/*Z* photoisomerization. Scheme 3 shows the process (*E*/*E*)-**1**⇆(*E*/*Z*)-**1**, which leads to a photostationary state. The (*Z*,*Z*) configuration is not included. (Detection limit below 2% in the ^{1}H NMR spectroscopy.) The reaction spectra of Figure 3 illustrate the obtention of the photostationary state of **1a**

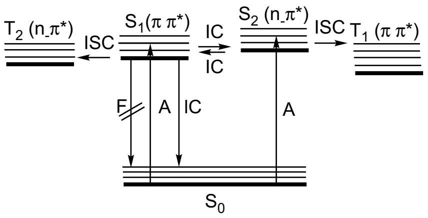

Figure 2. Term scheme of the (*E*,*E*)-3,6-bis(styryl)pyridazines **1**/**1′**. Absorption A, fluorescence F, internal conversion IC, intersystem crossing ISC.

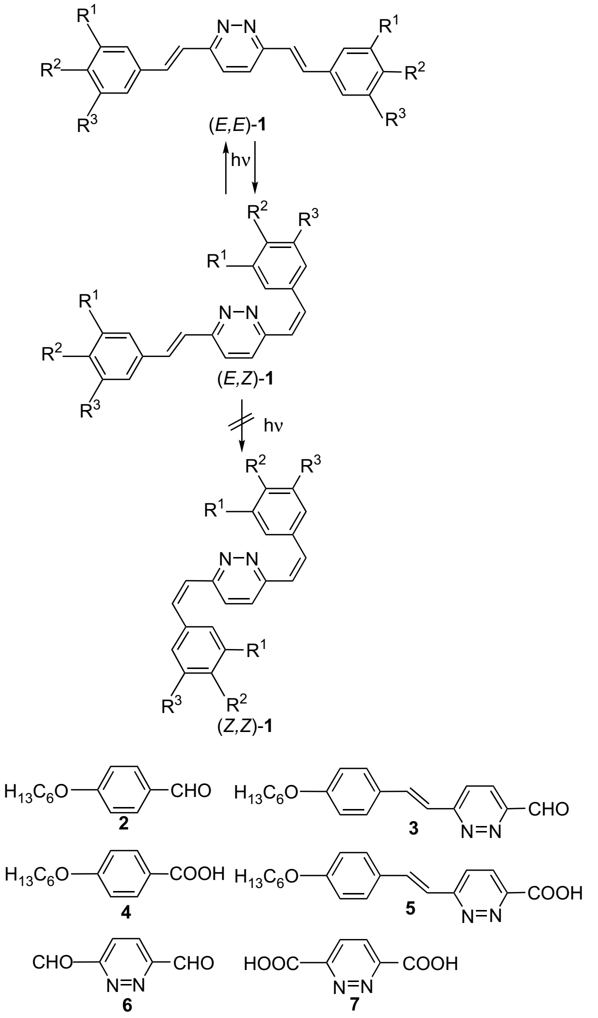

Scheme 3. Photoisomerization of (*E*,*E*)-**1**/(*E*,*Z*)-**1** and possible cleavage products of **1c** on irradiation in the presence of oxygen.

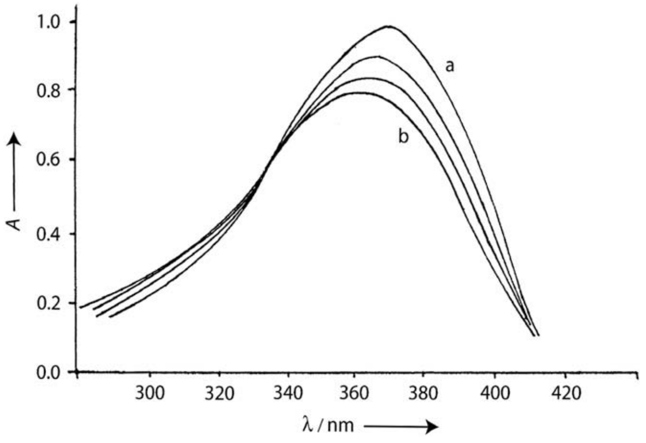

Figure 3. Reaction spectra of the irradiation of a 2×10^{-4} M solution of (*E*,*E*)-**1a** in oxygen-free benzene. The upper curve (a) corresponds to the start with pure (*E*,*E*) configuration, the lower curve (b) corresponds to the photostationary state (*E*,*E*)/(*E*,*Z*)=54:46.

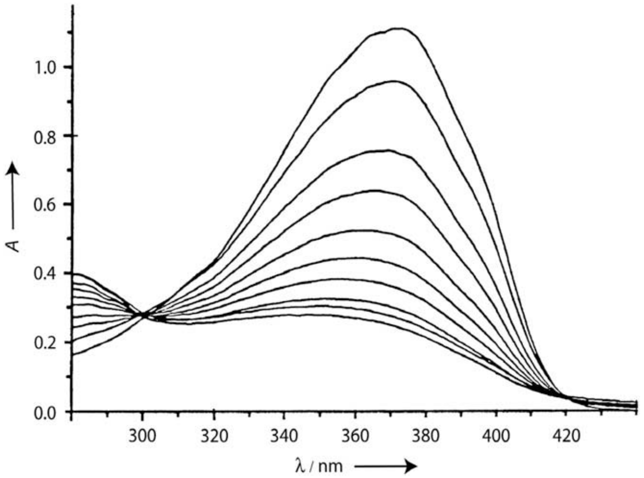

Figure 4. Reaction spectra (top to bottom) of the irradiation of a 2×10^{-4} M solution of (*E*,*E*)-**1a** in oxygen-containing benzene.

on irradiation with 366 nm in benzene in the absence of oxygen. The reaction spectra of Figure 4 demonstrate the complete decomposition of **1a** on irradiation in the presence of oxygen. Oxygen provokes a cleavage of the olefinic double bonds. Scheme 3 summarizes the possible cleavage products **2**–**7** derived from **1c**; FD MS spectroscopy proved the generation of 4-hexyloxy benzaldehyde (**2**), 4-hexyloxybenzoic acid (**4**), 6-[2-(4-hexyloxy phenyl)vinyl]pyridazine-3-carbaldehy-de (**3**) and its carboxylic acid **5**. Pyridazine-3,6-dicarbaldehyde (**6**) in and its 3,6-dicarboxylic acid (**7**) were not found, but the major reaction product is under this conditions a polymer, which may have **6** and **7** incorporated.

Our first assumption, that the cleavage of **1** can be due to the formation of singlet-oxygen with **1** as sensitizer according to Eq. 1, could not be verified.

$$S_0(\mathbf{1}) \xrightarrow{h\nu} S_{1,2}(\mathbf{1}) \xrightarrow{\text{ISC}} T_{2,1}(\mathbf{1}) \xrightarrow{+^3O_2} S_0(\mathbf{1}) + {}^1O_2 \longrightarrow \ldots \tag{1}$$

Thermal production of $^1O_2$ from 9,10-diphenylanthracene-*endo*-peroxide did neither give a 1,2-dioxetane of **1a** nor its cleavage products. Therefore, a radical process has to be postulated for the oxidative photodegradation of **1**.

The other pyridazines **1b**–**f** behave quite similar. So we carefully excluded O_2 in the photoisomerization experiments and determined the photostationary states of **1d**–**f** by irradiation of 2×10^{-4} M solutions in benzene with a medium pressure mercury lamp equipped with a Pyrex filter ($\lambda \geq 290$ nm). Table 2 shows the results, which were obtained by ^{1}H NMR measurements.

Interestingly the number of side chains has a considerable influence on the (*E*,*E*)/(*E*,*Z*) ratio. The 50:50 ratio of **1d** (two dodecyloxy chains) is changed for **1e** (four dodecyloxy chains) in favor of the (*E*,*E*) configuration and then for **1f** (six dodecyloxy chains) in the opposite direction in favor of the (*E*,*Z*) configuration. Since the absorption of **1d**–**f** is almost identical, the different isomerization tendencies may be due to a different participation of conformers.

The (*E*,*Z*)-isomers can be easily identified by their ^{1}H NMR spectra. In contrast to the (*E*,*E*)-isomers, the pyridazine ring represents in the (*E*,*Z*)-isomers an AB system instead of a singlet and the ^3J coupling constant of the olefinic protons on the (*Z*)-configured double bond is 12.3±0.2 Hz instead of 15.1±0.2 Hz for the (*E*)-configured double bond.

To obtain full ^{1}H and ^{13}C NMR characterization, we separated (*E*,*E*)-**1d**/-(*E*,*Z*)-**1d** by fractional crystallization. The component (*E*,*E*)-**1d** has a much lower solubility in benzene and can be filtered

Table 2
Photostationary states of the pyridazines **1a**,**d**–**f** obtained in 2×10^{-4} M solutions in benzene ($\lambda \geq 290$ nm)

Compound	1a	1d	1e	1f
(*E*/*E*)/(*E*/*Z*)	54:46	50:50	75:25	40:60

off. The remaining (*E*,*Z*)-**1d** is a colorless powder, which does not form a mesophase. A chromatographic separation on SiO_2 is not advisable because the catalytic (*E*,*Z*)→(*E*,*E*) isomerization enriches then the (*E*,*E*)-isomers.

Although we favored from the very beginning the triplet mechanism of the isomerization, a competitive by-road on the energy hypersurface of the excited singlet state cannot a priori be completely ruled out. Eq. 2 for the photostationary (*E*,*E*)/(*E*,*Z*) ratio takes this into account.

$$\frac{(E,E)}{(E,Z)} = \frac{\varepsilon_{EZ}\phi^{S}_{EZ\longrightarrow EE} + \phi^{S}_{ISC}(E,Z)\cdot\phi^{T}_{EZ\longrightarrow EE}}{\varepsilon_{EE}\phi^{S}_{EE\longrightarrow EZ} + \phi^{S}_{ISC}(E,E)\cdot\phi^{T}_{EE\longrightarrow EZ}} \qquad (2)$$

In order to find out if the singlet quantum yield $\phi^{S}_{EE\rightarrow EZ}$ for the isomerization (*E*,*E*)-**1f**→(*E*,*Z*)-**1f** can be neglected, we added azulene as a triplet quencher. Increasing amounts of azulene decreased dramatically the rate of (*E*,*Z*)-**1f** generation. A 7.2×10^{-3} M solution of (*E*,*E*)-**1f** in benzene, doped with a 7.2×10^{-2} M solution of azulene brought the isomerization to a complete stop. Therefore, $\phi^{S}_{EE\rightarrow EZ}$ can be neglected. When (*E*,*Z*)/(*E*,*E*) mixtures were applied for this experiment, the original isomer ratio is not preserved. A slow enrichment of the (*E*,*E*)-isomer can be observed—even for high azulene concentrations. The most likely explanation is that $\phi^{S}_{EZ\rightarrow EE}$ is small but not completely negligible. An alternative explanation would involve different efficiencies in the quenching of the triplet states of (*E*,*E*)-**1f** and (*E*,*Z*)-**1f**.

A final experiment in this context was performed with pyrene as triplet sensitizer. A $NiSO_4$ filter solution was used for a selective excitation of pyrene. It filters out the radiation in the absorption range of **1a**. A 2×10^{-4} M solution of (*E*,*E*)-**1a** in benzene, which contained 6×10^{-4} mol L^{-1} pyrene was irradiated and yielded the (*E*,*E*)-**1a**/(*E*,*Z*)-**1a** ratio of 50:50. This ratio corresponds fairly to the ratio 54:46 found in the absence of pyrene. Sensitized and direct photolyses have virtually the same result, because the isomerization is almost completely a triplet reaction. Scheme 4 summarizes the direct, sensitized, and quenched photoprocesses, which are valid for compounds **1**.

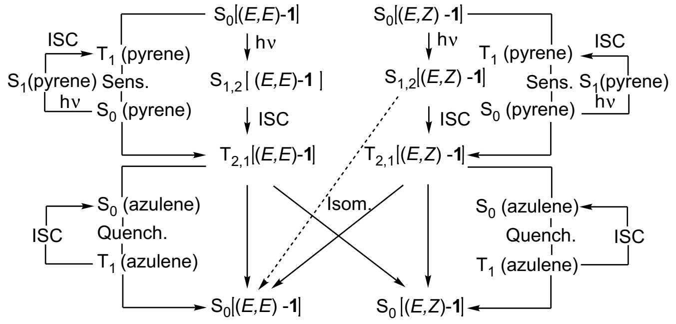

Scheme 4. Direct (h*ν*), sensitized (Sens.), and quenched (Quench.) photoreactions of 3,6-bis(styryl)pyridazines **1**, which effect isomerization (Isom.) and/or retention of the two involved configurations (*E*,*E*) and (*E*,*Z*).

2.3. Photochemistry of the LC phases

The crucial question is now: how can these photoisomerization processes be transferred from solution experiments to mesophases? The (*E*,*Z*) configuration does certainly not fit into any calamitic or phasmidic LC phase. A certain percentage of 'wrong' configuration may be tolerated, but soon a critical ratio (*E*,*Z*)-**1**/(*E*,*E*)-**1** should be reached, where the self-organization of the mesophase becomes impossible. This borderline between LC and I (Fig. 4) can be used in different mode for imaging and optical switching processes:

(a) Increasing photoisomerization (*E*,*E*)-**1**→(*E*,*Z*)-**1** will destruct the LC phase, provided that the photostationary state is lying in the range of the isotropic melt. The temperature for the transition LC→I (isotropic phase) can be significantly lowered in comparison to the pure mesophase.

(b) Irradiation of an isotropic phase I consisting of a mixture of (*E*,*E*)-**1** and (*E*,*Z*)-**1** will lead to the opposite 'border crossing', when the photostationary state is located in the LC region.

(c) The (*E*,*Z*)→(*E*,*E*) isomerization can principally work thermally or catalytically and thus transfer the isotropic phase to an LC layer, provided that the thermal (*E*,*E*)/(*E*,*Z*) equilibrium is in the LC range. Combination of the processes (a) and (c) represent another possibility of switching (or writing and erasing).

(d) The final borderline crossing process would consist of an increase of the (*E*,*Z*) configuration by thermal activation, till the LC phase breaks down. However, an LC phase at a temperature, where the thermal equilibrium is in the range of the isotropic melt, is principally unstable. Therefore, (d) is registered by a dashed line in Scheme 5.

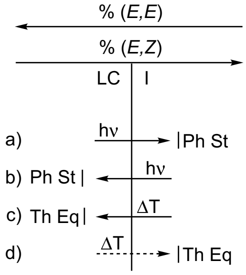

Scheme 5. Possible photochemical (cases (a) and (b)) and thermal (cases (c) and (d)) crossings of the borderline between LC phase and isotropic phase I depending on the position of the photostationary state (Ph St) and the thermal equilibrium (Th Eq) on the scale of (*E*,*E*) and (*E*,*Z*) isomers.

The dialkoxy substituted compounds **1a** and **1d** form thermotropic smectic (S) or nematic (N) phase. According to the second heating curve in the DSC, **1a** exists in the narrow temperature range between 161 and 170 °C in an $S_{F/I}$, between 170 and 283 °C in an S_C, and above 283 °C in an N phase.[2a] A similar behavior with somewhat lower transition temperatures was observed for **1d**, which contains two dodecyloxy groups (K–139 °C–$S_{F/I}$–168 °C–S_C–260 °C–I).[2a] All these mesophases do not allow an (*E*,*E*)→(*E*,*Z*) photoisomerization. Irradiation into the broad absorption band, which reaches from 250 to about 500 nm, exhibits photostability. Neither an exposure to daylight for many days nor an irradiation with $\lambda\geq320$ nm changes the materials. However, an irradiation ($\lambda\geq320$ nm) of an isotropic 50:50 mixture of (*E*,*Z*)-**1d** and (*E*,*E*)-**1d** at 150 °C leads very fast to the smectic phase $S_{F/I}$ with a content of (*E*,*Z*)-**1d** below 3%. Obviously, the photostationary state is far on the (*E*,*E*) side. A short heat shock to temperatures above 260 °C transforms the mesophase to the isotropic melt of pure (*E*,*E*)-**1d**. Compound **1a** shows an analogous photochemical behavior.

Compound **1b** has a sharp melting point at 128 °C (onset temperature in the DSC) and does not form liquid crystals. The same substitution pattern present in **1e**, but with $OC_{12}H_{25}$ instead of OC_6H_{13} chains, leads on cooling to the formation of a smectic phase: I–124 °C–S_A–106 °C–K.[2a] In contrast to the highly ordered smectic phases of **1a** and **1d**, compound **1e** forms an S_A phase, which has a much lower order and consequently can be degraded photochemically. The self-organization in the S_A phase allows the (*E*,*E*)-**1e**→(*E*,*Z*)-**1e** isomerization. Figure 5 shows the transition of the S_A phase at 122 °C to the isotropic phase on irradiation ($\lambda\geq320$ nm). Less than 3% of (*E*,*Z*)-**1e** provoke this transformation.

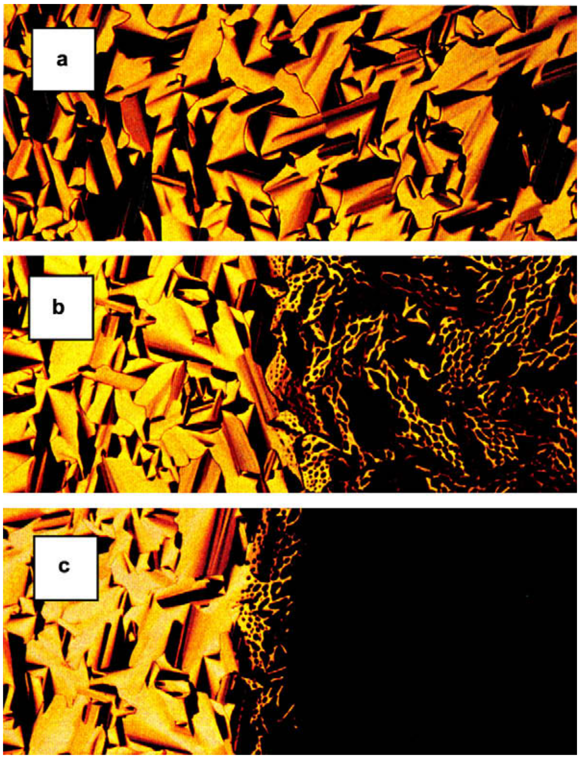

Figure 5. Degradation of the S_A phase of **1e** at 122 °C in the irradiated right part. (polarization microscopy, scale 1:90).

Interestingly a short annealing of the probe restores the S_A phase. Since a thermal isomerization (*E*,*Z*)-**1e**→(*E*,*E*)-**1e** is not possible under these conditions, we assumed either a catalytic isomerization or the separation of the (*E*,*Z*)-**1e** molecules on the domain borders.

The (*E*,*Z*) stereoisomers of **1** can be transformed in solution to the thermodynamic equilibrium by the action of acids. Therefore, we prepared LC phases of mixtures of (*E*,*E*)-**1e** and the organic acids **8**[14–18] or **9**,[19–21] which form themselves mesophases (Scheme 6).

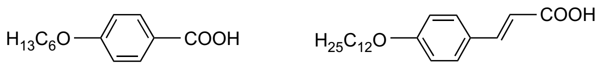

8 **9**

I—153 °C—S_C—105 °C—K I—162°C—N—156 °C—S_C—125 °C—K

Scheme 6. Smectic (S_C) and nematic (N) phases of 4-hexyloxybenzoic acid (**8**) and 4-dodecyloxycinnamic acid (**9**).

Up to 5% **8** and 10% **9** were mixed with (*E*,*E*)-**1e** in the molten state. Although **8** and **9** generate in pure form S_C phases, the mixtures enter a self-organization of the S_A type.[22] The single difference between these mixed S_A phases and the S_A phase of neat **1e** is a minor lowering of the phase transition temperatures ($\Delta T<4$ °C). Irradiation of the mixed S_A phases gave the same results as for the pure phase of **1e**. Photodegradation of the S_A phases occurred, when a small amount ($\leq$3%) of (*E*,*Z*)-**1e** was formed. The restoration of the S_A phase by annealing was not accelerated by the present acids. Therefore, we assume that the major effect of the annealing is that the 'wrong' (*E*,*Z*) configurations are ousted to the domain borders. The turnover S_A/I/S_A can be repeated several times, because the (*E*,*Z*) configurations are 'repaired' in the next irradiation period. A handicap of this writing-erasing technique is due to the fact that temperatures of about 120 °C are needed for the use of the S_A phase. Moreover, we found that the repair mechanism is not perfect, so that the system fatigues. An isotropic mixture, which contains 20% (*E*,*Z*)-**1e** and 80% (*E*,*E*)-**1e** cannot be transformed to the S_A phase – neither by irradiation nor by annealing. The amount of 'wrong' configuration is probably then too high for the ousting in border areas of LC domains and the photostationary ratio (*E*,*E*)-**1e**/(*E*,*Z*)-**1e** is obviously not sufficient for the photochemical generation of a mesophase.

Figure 6. Imaging technique by irradiation ($\lambda\geq320$ nm, $T=40$ °C) of a isotropic mixture (*E*,*E*)-**1f**/(*E*,*Z*)-**1f** (black area) through a mask. Polarization microscopy shows the birefringent areas, where the S_A phase was photochemically induced.

Both drawbacks are not valid for the hexa-substituted, phasmidic compounds **1c** and **1f**. They form S_A phases at room temperature[2a] and irradiation of isotropic (*E*,*E*)/(*E*,*Z*) mixtures with a high content of (*E*,*Z*) configuration (60%) furnishes LC phases. ^{1}H NMR measurements revealed that the photochemical transformation of a 40:60-mixture of (*E*,*E*)-**1f**/(*E*,*Z*)-**1f** at 30 °C to a 80:20-mixture is sufficient for the generation of a tight LC phase. Figure 6 demonstrates the use of this process for information storage. A film negative of the word 'cher' served as mask for the irradiation ($\lambda\geq320$ nm) at 40 °C. The letters have a thickness of about 50 μm. The resolution limit is in the range of 10 μm. A short heat shock to 80 °C provokes the erasing of the picture by formation of the isotropic phase. Pure (*E*,*E*)-**1f** has the clearing point of the S_A phase at 84 °C.[2a]

The photochemical induction of the S_A phase is possible, because the photostationary state of **1f** is in the S_A phase. That means on the other side, that a photodegradation of the S_A phase by the isomerization (*E*,*E*)-**1f**→(*E*,*Z*)-**1f** is not possible. Long-term irradiations of the isotropic phase reveal some fatigue because of the formation of oligomers. The S_A phase is photostable—even at temperatures relatively close to the clearing point, where the viscosity is lowered.

3. Conclusion

The 3,6-bis(styryl)pyridazines **1a** and **1d**, which bear two alkoxy side chains, represent case (b) of Scheme 5. The photostationary state is in the LC range, so that the mesophase can be induced by irradiation of an isotropic (*E*,*E*)/(*E*,*Z*) mixture, but the mesophase cannot be photodegraded. The tetrasubstituted system **1e** behaves opposite.[23] Corresponding to type (a) of Scheme 5, the self-organization of the S_A phase can be photochemically destroyed, but not induced, because the photostationary state lies in the range of the isotropic melt. Most suitable for imaging techniques are the S_A phases of **1c** and **1f**, because they exist at room temperature. As for **1a** and **1d**, the generation of a mesophase by partial photoisomerization (*E*,*Z*)→(*E*,*E*) is possible, since the photostationary state is located in the LC range of the (*E*,*E*)/(*E*,*Z*) ratio. After the 'writing' process an 'erasing' is possible by a short heat shock. Thermal or catalytic isomerization (*E*,*E*)-**1**$\leftrightarrows$(*E*,*Z*)-**1** [cases (c) and (d) of Scheme 5] could be excluded under the conditions used here.

4. Experimental

4.1. General

Melting points were determined on a Büchi 510 melting point apparatus and are uncorrected. The DSC measurements were performed on a Perkin–Elmer DSC 7. IR spectra were measured with a Beckman Acculab spectrometer. A Zeiss MCS 224/234 diode array spectrometer was used for the UV–vis spectroscopy. The Bruker spectrometer AC 200 and AM 400 served for the measurement of the ^{1}H and ^{13}C NMR spectra. $CDCl_3$ was used as solvent and TMS as internal standard. The mass spectra were obtained on a Finnigan MAT 95. Polarization microscopy was performed with a Leitz Ortholux II microscope and a Mettler FP-52 heating system.

4.2. Synthesis of the 3,6-bis(styryl)pyridazines 1a–f and the carboxylic acids 8 and 9

The preparation of (*E*,*E*)-**1a**–**f**,[2a] **8**,[14–18] and **9**[19–21] was described earlier.

4.3. Irradiations in solution

For analytical purposes, irradiations were performed in quartz cuvettes with an Osram XBO-1000 W OFR high-pressure Xenon lamp in an AMKO device. The monochromator was adjusted to 320 or 366 nm. That corresponds to the two maxima in the continues emission of the lamp between 300 and 800 nm. A water filter served for the absorption of the IR radiation, so that the solutions in oxygen-free benzene were kept at room temperature. The UV–vis spectra were measured in a direction perpendicular to the irradiation beam.

For preparative purposes a Hanovia 450-W medium pressure lamp, equipped with a Pyrex filter ($\lambda \geq 290$ nm), was used. Solutions of **1** (180 mL, 2.0×10^{-4} mol L^{-1} in oxygen-free benzene) were irradiated in an immersion vessel under vigorous stirring in an Ar atmosphere. A cooling system between lamp and solution was regulated between 25 and 70 °C, so that clear solutions without precipitation were maintained.

The photostationary states of **1a**,**d**–**f** (Table 2) were determined by ^{1}H NMR measurements with repeated and averaged integration.

The quenching experiments were performed with a 7.2×10^{-3} M solution of (*E*,*E*)-**1f** in benzene to which increasing amounts of azulene were added. When the tenfold concentration (7.2×10^{-2} M) of azulene was reached, the isomerization (*E*,*E*)→(*E*,*Z*) came to a complete stop.

For the triplet-sensitized photoreaction, a 2.0×10^{-4} M solution of (*E*,*E*)-**1a** in benzene was used, which contained 6.0×10^{-4} mol L^{-1} pyrene. The cooling system was filled with an aqueous solution of $NiSO_4\cdot6H_2O$ (300 g L^{-1}). A thickness of about 1 cm of the $NiSO_4$ solution ensured that the light between 320 and 480 nm was filtered off, so that the incident light between 290 and 320 nm was selectively absorbed by pyrene.

4.3.1. (E,Z)-3,6-Bis[2-(4-dodecyloxyphenyl)-vinyl]pyridazine (E,Z)-1d

The preparative irradiation described above yielded a 1:1-mixture (23.5 mg) of (*E*,*E*)-**1d** and (*E*,*Z*)-**1d**. UV–vis spectroscopy indicated after about 4 h the photostationary state. The isomer ratio was determined by ^{1}H NMR spectroscopy. Repeated fractional crystallization from benzene permitted the separation of the two stereoisomers, because the (*E*,*Z*)-isomer is much better soluble. Pure (*E*,*E*)-**1d** is a yellow powder, which melts at 139 °C to the smectic phase.[2a] Pure (*E*,*Z*)-**1d** is a pale yellow powder, which starts to decompose above 120 °C. ^{1}H NMR (400 MHz, $CDCl_3$): δ 0.86 (t, 6H, CH_3), 1.24 (m, 32H, CH_2), 1.45 (m, 4H, CH_2), 1.85 (m, 4H, CH_2), 3.92 (t, 2H, OCH_2), 3.99 (t, 2H, OCH_2), 6.78/7.21 (AA′BB′, 4H, aromat. H, (*Z*) side), 6.82/6.92 (AB, ^3J=12.4 Hz, 2H, olefin. H, (*Z*) configuration), 6.89/7.50 (AA′BB′, 4H, aromat. H, (*E*) side), 7.19/7.51 (AB, ^3J=16.2 Hz, 2H, olefin. H, (*E*) side), 7.24/7.31 (AB, ^3J=8.9 Hz, 2H, heteroarom. H).[24] ^{13}C NMR (100 MHz, $CDCl_3$): δ 14.1 (CH_3), 22.7, 26.0, 29.3, 29.4, 29.6, 29.6, 29.7, 29.7, 31.9 (CH_2, partly superimposed), 68.1, 68.2 (OCH_2), 114.5, 114.9, 122.4, 123.0, 126.3, 126.6, 128.7, 130.2, 134.3, 135.0 (aromat. and olefin. CH), 128.5, 128.5, 156.4, 157.3, 159.1, 160.0 (aromat. C_q). FD MS: *m*/*z* (%) 652 (100) [$M^{+\bullet}$]. Anal. Calcd for $C_{44}H_{64}N_2O_2$ (653.0): C 80.93, H 9.89, N 4.29; found: C 81.13, H 10.00, N 4.12.

4.3.2. Photooxidative degradation of (E,E)-3,6-bis[2-(4-hexyloxyphenyl)vinyl]pyridazine (1a)

A solution of **1a** (17.4 mg, 0.036 mmol) in 185 mL dry benzene was irradiated at 30 °C with a Hanovia 450 W medium pressure lamp, equipped with a Pyrex filter ($\lambda \geq 290$ nm). During the irradiation of 3.5 h a stream of air was purged through the solution. UV–vis spectroscopy indicated the consumption of the starting compound. The solvent was evaporated and the mixture subjected to a FD MS analysis, which revealed the presence of **1a**: *m*/*z* 484 [$M^{+\bullet}$], 4-hexyloxybenzaldehyde (**2**): *m*/*z* 206 [$M^{+\bullet}$], 6-[2-(4-hexyloxyphenyl)vinyl]pyridazine-3-carbaldehyde (**3**): *m*/*z* 310 [$M^{+\bullet}$], 4-hexyloxybenzoic acid (**4**): *m*/*z* 222 [$M^{+\bullet}$], and 6-[2-(4-hexyloxyphenyl)vinyl]pyridazinecarboxylic acid (**5**): *m*/*z* 326 [$M^{+\bullet}$]; **2** as a daughter ion of **4** and **3** as a daughter ion of **5** could be excluded. The peak intensities do not represent the real amounts of the ions were: **1a**/**2**/**3**/**4**/**5**=6:100:21:21:4. The ^{1}H NMR spectrum of the reaction mixture revealed that **2** was the major product (10%) of low molecular weight. About 80% are oligomeric products.

The reaction of **1a** with 9,10-diphenylanthracene-9,10-*endo*-peroxide[25] did neither give a 1,2-dioxetane of **1a** nor the cleavage products **2**–**5**. Apart from unreacted **1a**, only oligomers of undefined structure were generated.

4.4. Irradiation of the LC phases

Isotropic melts (25 mg) of the LC forming compounds were used to generate films between two Duran glass plates ($\lambda \geq 310$ nm). The irradiations were performed with an UVGL-58 lamp, whose emission lies between 320 and 400 nm with a maximum at 352 nm. A Digsitherm DT-3434 heating system kept the temperature on the desired level (accuracy ±1 °C). The following conditions were used:

(a) (*E*,*E*)-**1a**: 290 °C (N), 200 °C (S_C), 165 °C ($S_{F/I}$).
(b) (*E*,*E*)-**1d**: 250 °C (S_C), 200 °C (S_C), 145 °C ($S_{F/I}$).

During the irradiation up to 150 min, all phases were kept intact and the ^{1}H NMR spectra of the irradiated films (dissolved in $CDCl_3$ or C_6D_6) did not contain any signals of (*E*,*Z*) configurations.

(c) (*E*,*E*)-**1d**/(*E*,*Z*)-**1d** (50:50): 150 °C (I).

After 1 min irradiation, the $S_{F/I}$ phase was formed, and the ^{1}H NMR spectrum revealed that the content of (*E*,*Z*)-**1d** was below 3%. A short heat shock to temperatures above 260 °C led to the isotropic melt. (*E*,*E*)-**1a** exhibits the same behavior.

(d) (*E*,*E*)-**1e**: 122 °C (S_A), 140 °C (I).

The smectic phase disappeared quickly, before 3% (*E*,*Z*) configuration was formed. Long-term irradiations (10–90 min) of S_A or irradiations of the isotropic melt (I) led to an appreciable amount of oligomers up to 20%. Irradiation of a crystalline film for 90 min at 110 °C revealed a complete photostability.

(e) (*E*,*E*)-**1c** and (*E*,*E*)-**1f**: 25 °C (S_A).

The S_A phases are photostable. Long-term irradiations (60–120 min) led to the formation of 10% dimer and oligomers.

(f) (*E*,*E*)-**1f**/(*E*,*Z*)-**1f** (40:60): 20 °C, 30 °C, 40 °C.

Irradiation led immediately to an enrichment of the (*E*,*E*)-isomer. After a few minutes the S_A phase was formed. ^{1}H NMR measurement revealed that a ratio of 80% (*E*,*E*)-**1f** and 20% (*E*,*Z*)-**1f** is already sufficient for a high-quality texture. Long-term irradiation showed some fatigue due to dimerization (6%). A short heat shock to 80 °C erased the texture, but did not change the (*E*,*E*)/(*E*,*Z*) ratio.

Acknowledgements

We are grateful to the Deutsche Forschungsgemeinschaft, the Fonds der Chemischen Industrie and the Centre of Materials Science of the University of Mainz.

References and notes

1. Selected monographs and reviews: (a) Grimsdale, A. C. In *Organic Light-Emitting Devices*; Müllen, K., Scherf, U., Eds.; Wiley-VCH: Weinheim, 2006; pp 215–243; (b) Meier, H. In *Carbon-Rich Compounds*; Haley, M. M., Tykwinski, R. R., Eds.; Wiley-VCH: Weinheim, 2006; (c) Hadziioannou, G.; van Hutten, P. F. *Semiconducting Polymers*; Wiley-VCH: Weinheim, 2000; (d) Segura, J. L.; Martin, N. *J. Mater. Chem.* **2000**, *10*, 2403–2435; (e) Martin, R. E.; Diederich, F. *Angew. Chem.* **1999**, *111*, 1440–1469; *Angew. Chem., Int. Ed.* **1999**, *38*, 1350–1377; (f) Scherf, U. *Top. Curr. Chem.* **1999**, *201*, 163–222; (g) Müllen, K.; Wegner, G. *Electronic Materials: The Oligomer Approach*; Wiley-VCH: Weinheim, 1998; (h) Kraft, A.; Grimsdale, A. C.; Holmes, A. B. *Angew. Chem.* **1998**, *110*, 416–443; *Angew. Chem., Int. Ed.* **1998**, *37*, 403–428; (i) Tour, J. M. *Chem. Rev.* **1996**, *96*, 537–553.
2. See, for example: (a) Lifka, T.; Zerban, G.; Seus, P.; Oehlhof, A.; Meier, H. *Tetrahedron* **2008**, *64*, 6551–6560; (b) Stadler, A.-M.; Puntoriero, F.; Campagna, S.; Kyritsakas, N.; Welter, R.; Lehn, J.-M. *Chem.—Eur. J.* **2005**, *11*, 3997–4009; (c) Van der Eycken, E.; Jidong, Z.; Kilonda, A.; Compernolle, F.; Toppet, S.; Moornaert, G.; Van der Auweraer, M.; Jackers, C.; Verbouwe, W.; De Schryver, F. C. *J. Chem. Soc., Perkin Trans. 2* **2002**, 928–937; (d) Eynde, J. J. V.; Pascal, L.; Van Haverbeke, Y.; Dubois, P. *Synth. Commun.* **2001**, *31*, 3167–3174; (e) Brooker, S.; Kelley, R. *J. Chem. Soc., Dalton Trans.* **1996**, 2117–2122; (f) Nohara, M.; Hasegawa, M.; Hosokawa, C.; Tokailin, H.; Kusumoto, T. *Chem. Lett.* **1990**, *2*, 189–190.
3. Dorohoi, D.; Partenie, H.; Chiran, L.; Anton, C. *J. Chim. Phys. Phys. Chim. Biol.* **1994**, *91*, 419–432.
4. Perkampus, H. H.; Bluhm, T.; Knop, J. V. *Spectrochim. Acta, A* **1972**, *28*, 2163–2177.
5. El-Sayed, M. A. *J. Chem. Phys.* **1962**, *36*, 573–574.
6. El-Sayed, M. A. *J. Chem. Phys.* **1964**, *41*, 2462–2467.
7. Meier, H. *Angew. Chem.* **1992**, *104*, 1425–1446; *Angew. Chem., Int. Ed. Engl.* **1992**, *31*, 1399–1420.
8. Sandros, K.; Sundahl, M.; Wennerström, O.; Norinder, U. *J. Am. Chem. Soc.* **1990**, *112*, 3082–3086.
9. Meier, H. *Angew. Chem.* **2005**, *117*, 2536–2561; *Angew. Chem., Int. Ed.* **2005**, *44*, 2482–2506.
10. Meier, H.; Lifka, T.; Stalmach, U.; Oehlhof, A.; Prehl, S. *Eur. J. Org. Chem.* **2008**, 1568–1574.
11. Oelkrug, D.; Tompert, A.; Egelhaaf, H.-J.; Hanack, M.; Steinhuber, E.; Hohloch, M.; Meier, H.; Stalmach, U. *Synth. Met.* **1996**, *83*, 231–237.
12. The measured as well as the calculated electron excitation energies are lowest for the tetrasubstituted compounds **1b**,**e**/**1′b**,**e′**.
13. Moreover, the energetical sequence of close lying singlet states S_1/S_2 or triplet states T_1/T_2 can depend on the solvent (medium).
14. Malthête, J.; Canceill, J.; Gabard, J.; Jacques, J. *Tetrahedron* **1981**, *37*, 2815–2821.
15. Coco, S.; Espinet, P.; Marcos, E. *J. Mater. Chem.* **2000**, *10*, 1297–1302.
16. Kim, B. G.; Kim, S.; Park, S. Y. *Mol. Cryst. Liq. Cryst. Sci. Technol., Sect. A* **2001**, *370*, 391–394.
17. Prajapati, A. K.; Sharma, H. C.; Chudgar, N. K. *Mol. Cryst. Liq. Cryst.* **2001**, *364*, 815–824.
18. Prajapati, A. K.; Pandya, H. M. *Mol. Cryst. Liq. Cryst. Sci. Technol., Sect. A* **2003**, *393*, 31–40.
19. Tuffin, R. P.; Goodby, J. W.; Bennemann, D.; Heppke, G.; Loetzsch, D.; Scherowsky, G. *Mol. Cryst. Liq. Cryst. Sci. Technol., Sect. A* **1995**, *260*, 51–68.
20. Lifka, T.; Meier, H. *J. Prakt. Chem./Chem.-Ztg.* **1995**, *337*, 641–646 and references therein.
21. Prajapati, A. K.; Thakkar, U.; Bonde, N. *Mol. Cryst. Liq. Cryst. Sci. Technol., Sect. A* **2003**, *393*, 41–48.
22. Higher contents of **8** and **9** in these mixtures lead to phase separation.
23. The other tetrasubstituted compound **1b** does not form a mesophase.
24. Assignemnt by INDOR measurements.
25. Wassermann, H. H.; Scheffer, J. R.; Cooper, J. L. *J. Am. Chem. Soc.* **1972**, *94*, 4991–4996.